Neuromusculoskeletal human multibody models for the gait of healthy and spinal-cord-injured subjects

Florian Michaud

Doctoral thesis

Ferrol, January 23rd, 2020

UNIVERSIDADE DA CORUÑA

Outline

Outline

Motivation

- Premature death, secondary conditions, low integration, high costs.
- Standing up and walking regularly has huge benefits for the general health state of these subjects.
- Assistive devices maximize: function, independence, well-being, integration.

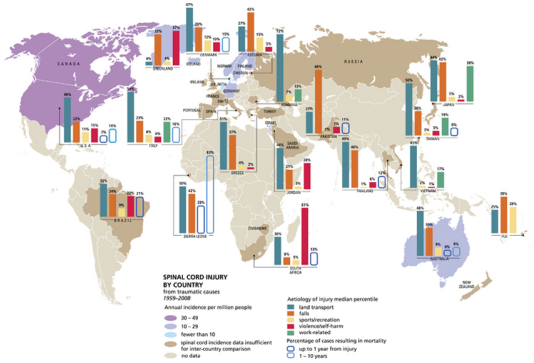

500,000 new SCI people/year due to land transport, falls, sport, violence, work, etc.

Motivation

This thesis has been developed in the context of a national project with the following objectives:

- Design of a low-cost active knee-ankle-foot orthosis (KAFO) for the gait of SCI subjects.
- Development of analysis methods to support orthosis design and patient adaptation.

Gait analysis

- Natural mode of locomotion of the adult human being.
- Multibody models and motion capture.
- Inverse and forward dynamics analysis at skeletal level.
  - Need to distribute the ground reaction forces during multiple ground contact.

Gait analysis

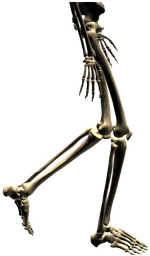

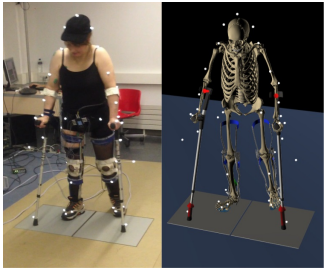

- Natural mode of locomotion of the adult human being.
- Multibody models and motion capture.
- Inverse and forward dynamics analysis at skeletal level.
  - Need to distribute the ground reaction forces during multiple ground contact.

Gait analysis


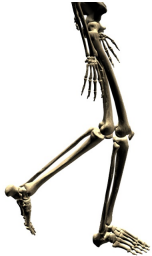


- Knowledge of muscle forces and other magnitudes from muscle dynamics are essential to:
  - Correctly determine joint reactions.
  - Open the way to estimate energetic cost and bone stress and strain.
  - Evaluate the impact of assisted gait in the health of SCI subjects and compare different assistive devices.

Neuromusculoskeletal modeling

- Muscle geometries and properties.
  - Number of muscles.
  - Model of muscle wrapping.
  - Location of the insertion points.
  - Maximal forces and optimal lengths.
- Musculotendon actuator dynamics.
  - Physiological behaviour.
- Central nervous system (CNS) strategy.
  - Muscle force-sharing problem.

Objectives

Therefore, the present work is devoted to:

- Review, select, adapt, improve and/or develop, and validate, all the necessary methods and tools which are required for gait analysis of healthy and spinal-cord-injured subjects:
  - Personalized musculoskeletal models.
  - Methods for analysis at skeletal and musculoskeletal levels.
  - Methods for energetic cost estimation.
- Apply them to two SCI subjects, bilateral and unilateral, respectively, and to compare a new active KAFO with a conventional passive one.

Outline

Subjects

The gait of 5 voluntary healthy subjects were recorded for the experimental validation of the different methods treated in this work.

	Subjects				
	1	2	3	4	5
Gender	Male	Male	Male	Female	Male
Age	28	26	58	30	28
Weight (kg)	86	74	96	50	99
Height (cm)	187	182	190	165	180
Speed (m/s)	1,18	1,29	1,14	0,92	1,20

Skeletal model

The human body is modeled as a 3D multibody system formed by rigid bodies.

- 18 anatomical segments linked by ideal spherical joints.
- 57 degrees of freedom (DOFs).
  - 18 sets of 3 angles plus 3 pelvis translations.
- Kinematic information of the motion obtained from the trajectories of the 37 optical markers attached to the subject's body.

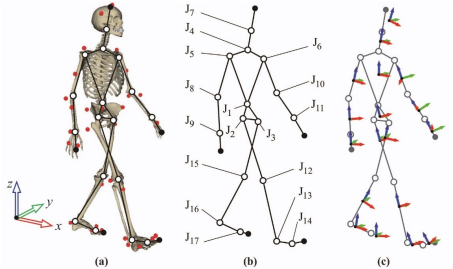

Musculoskeletal model

Gait studies for healthy people focus on lower limbs.

- 43 muscles are considered in each leg of the model plus 6 muscles in the pelvis.
- Geometries and properties of muscles are taken from OpenSim and scaled to the subjects.
  - Scott L. Delp, Frank C. Anderson, Allison S. Arnold, Peter Loan, Ayman Habib, Chand T. John, Eran Guendelman, and Darryl G. Thelen. Opensim: Opensource software to create and analyze dynamic simulations of movement. IEEE Trans. Biomed. Engineering, 54(11):1940-1950, 2007.

OpenSim

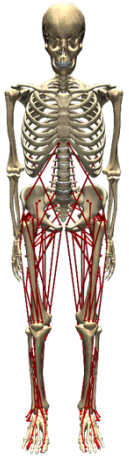

Muscle paths

The musculotendon length, musculotendon velocity, and moment arms of a muscle depend directly on the musculoskeletal geometry as well as on body segment configurations.

- Muscles are modeled as a single or a multiple straight line with several points.
- These points correspond to the attachment of the muscle to the bone and are defined as origin (i.e., proximal attachment) and insertion (i.e., distal attachment).
- Moment arms of muscles are calculated from the effective origin and the effective insertion which define the line of action of the muscle.

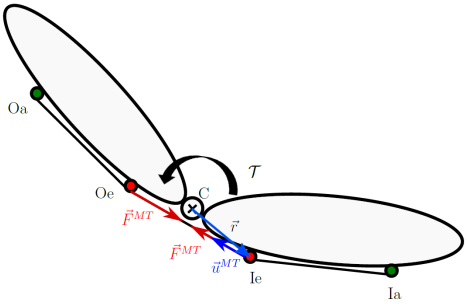

Musculotendon actuator dynamics

The dynamics of musculotendon actuators can be divided into:

Musculotendon actuator dynamics

The dynamics of musculotendon actuators can be divided into:

- Activation dynamics.
  - Transformation of a neural excitation into an activation of the contractile apparatus.

$$a = f(u) \tag{1}$$

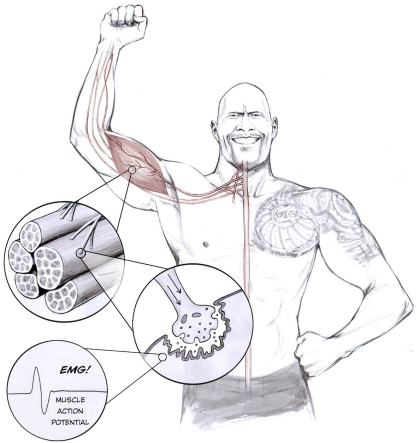

Musculotendon actuator dynamics

The dynamics of musculotendon actuators can be divided into:

- Activation dynamics.
  - Transformation of a neural excitation into an activation of the contractile apparatus.

$$a = f(u) \tag{1}$$

- Contraction dynamics.
  - Transformation of the activation into a muscle force.

$$F^{MT} = f(a) \tag{2}$$

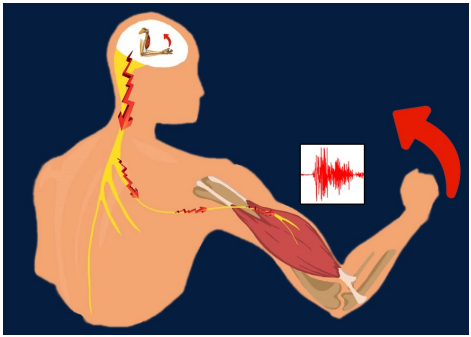

Activation dynamics

Activation dynamics is described by an ordinary first-order differential equation that contains the relationship among the muscle activation $a = a(t)$, its derivative $\dot{a} = \dot{a}(t)$, and the neural excitation $u = u(t)$ as

$$\dot{a} = (u-a)\frac{u}{\tau_{act}} + [u-(a-a_{min})-(u-a)u]\frac{1}{\tau_{deact}} \quad (3)$$

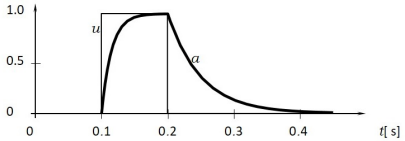

Hill's muscle model

The simplified mechanical model of a musculotendon consists of an active contractile element (CE), a parallel passive elastic element (PE), and a serial elastic element (SE).

- Felix E. Zajac. Muscle and tendon: properties, models, scaling, and application to biomechanics and motor control. Critical Reviews in Biomedical Engineering, 17:359-411, 1989.

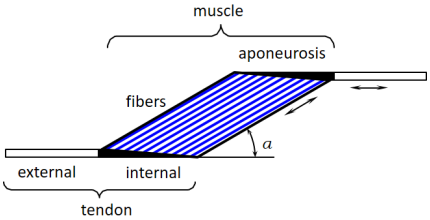

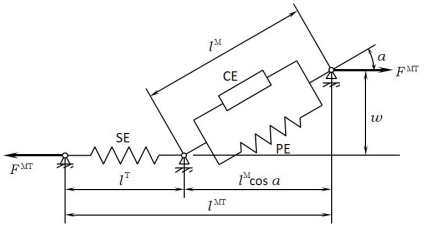

Hill's muscle model

$$F^{MT} = (F^M_{CE} + F^M_{PE}) \cos\alpha = F^M_0 \cdot f_T(\varepsilon^T). \qquad (4)$$

Muscle Tendon

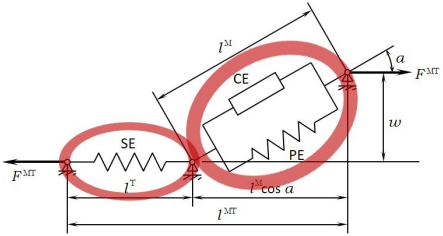

Hill's muscle model

$$F^{MT} = (F^M_{CE} + F^M_{PE}) \cos\alpha = F^M_0 \cdot f_T(\varepsilon^T). \quad (4)$$

(Muscle: $F^M_{CE} + F^M_{PE}$; Tendon: $f_T(\varepsilon^T)$)

$$F^M_{CE} = F^M_0 \cdot a \cdot f_l(\tilde{l}^M) \cdot f_v(\tilde{v}^M) \quad (5)$$

$$F^M_{PE} = F^M_0 \cdot f_{PE}(\tilde{l}^M) \quad (6)$$

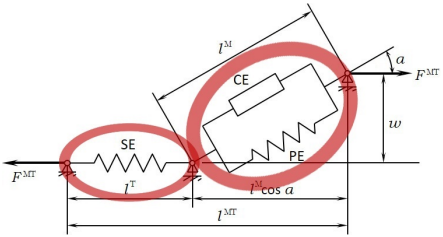

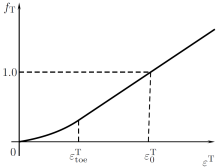

Force-strain curve of tendon

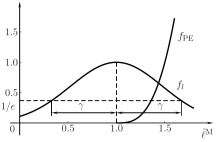

Force-length curves of the contractile and passive elements

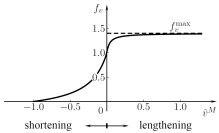

Force-velocity curve of contractile element

Hill's muscle model

$$F^{MT} = (F^M_{CE} + F^M_{PE}) \cos\alpha = F^M_0 \cdot f_T(\varepsilon^T). \quad (4)$$

(Muscle: $F^M_{CE} + F^M_{PE}$; Tendon: $f_T(\varepsilon^T)$)

$$F^M_{CE} = F^M_0 \cdot a \cdot f_l(\tilde{l}^M) \cdot f_v(\tilde{v}^M) \quad (5)$$

$$F^M_{PE} = F^M_0 \cdot f_{PE}(\tilde{l}^M) \quad (6)$$

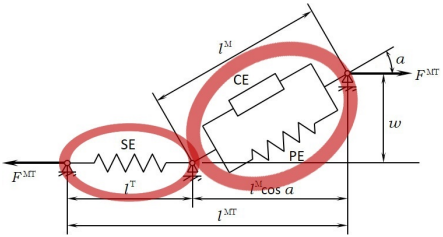

$$\dot{F}^{MT} = k^T \left[v^{MT} - \frac{v_{max}}{\cos\alpha} f_v^{-1} \left(\frac{F^{MT}/\cos\alpha - F^M_0 \cdot f_{PE}(l^M)}{F^M_0 \cdot a \cdot f_l(l^M)} \right) \right] \quad (7)$$

Hill's muscle model

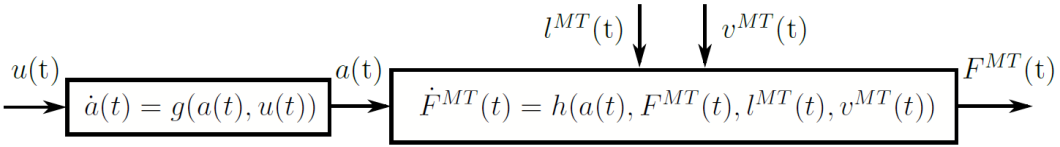

Hill's muscle model

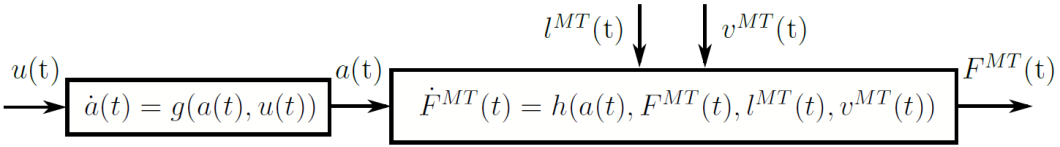

$$\dot{x}(t) = \begin{bmatrix} \dot{a}(t) \\ \dot{F}^{MT}(t) \end{bmatrix} = \begin{bmatrix} g(a(t), u(t)) \\ h(a(t), F^{MT}(t), l^{MT}(t), v^{MT}(t)) \end{bmatrix}. \tag{8}$$

$$\dot{x}(t) = f(x(t), u(t), l^{MT}(t), v^{MT}(t)) \tag{9}$$

Hill's muscle model

This system is used to define the limits of the optimization problem:

$$x_{i,min}(t_k) = x_i(t_{k-1}) + \int_{t_{k-1}}^{t_k} f(x_i(t), u_{i,k-1}(t) = 0, l_i^{MT}(t), v_i^{MT}(t))\, dt, \quad (10)$$

$$x_{i,max}(t_k) = x_i(t_{k-1}) + \int_{t_{k-1}}^{t_k} f(x_i(t), u_{i,k-1}(t) = 1, l_i^{MT}(t), v_i^{MT}(t))\, dt. \quad (11)$$

Time integrations of muscle equations are carried out using the ode23t integrator of Matlab (implicit trapezoidal rule).

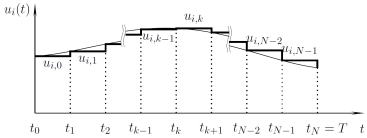

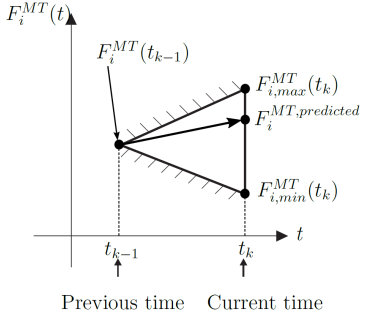

Hill's muscle model with rigid tendon

- Optimization and integration are both heavy and slow calculation processes.
  - Programming the muscle equations into a Mex file in Fortran language reduces the computational time by 10.
- The high tendon stiffness makes really difficult to use this approach.
- Most authors prefer to use a Hill-type musculotendon model with a rigid tendon.

In this way, the tendon length is constant:

$$l^T = l_S^T$$

Consequently, it is obtained:

$$v^M = v^{MT} \cos\alpha$$

Hill's muscle model with rigid tendon

Use of the rigid tendon model avoids the two integrations needed to calculate the limits of the muscle force at each instant.

Time response ignored (Phys. 2) - *direct relation*
Usually, authors who consider the tendon as a rigid element ignore the muscular time response and assume that:

$$a(t_k) = u_k \tag{12}$$

Consequently:

$$F^{MT}_{min} = F^{M}_{PE} \cdot \cos\alpha \tag{13}$$

$$F^{MT}_{max} = (F^{M}_{0} \cdot f_l(\tilde{l}^M) \cdot f_v(\tilde{v}^M) + F^{M}_{PE}) \cdot \cos\alpha \tag{14}$$

Hill's muscle model with rigid tendon

Time response considered (Phys. 3) - *differential equation*

In order to keep the muscular time response relation, the analytical solution of the first-order ordinary differential equation is used:

$$a(t_k) = \begin{cases} u_k + (a(t_{k-1}) - u_k) \cdot e^{(-dt/\tau_{act})} & \text{if} \quad a(t_{k-1}) < u_k \\ u_k + (a(t_{k-1}) - u_k) \cdot e^{(-dt/\tau_{deact})} & \text{if} \quad a(t_{k-1}) \geq u_k \end{cases} \tag{15}$$

Therefore, the minimum and maximum muscle activations, a_{min} ($u = 0$) and a_{max} ($u = 1$) can be obtained, and the muscle force limits become:

$$F^{MT}_{min} = (F^M_0 \cdot a_{min} \cdot f_l(\tilde{l}^M) \cdot f_v(\tilde{v}^M) + F^M_{PE}) \cdot \cos\alpha \tag{16}$$

$$F^{MT}_{max} = (F^M_0 \cdot a_{max} \cdot f_l(\tilde{l}^M) \cdot f_v(\tilde{v}^M) + F^M_{PE}) \cdot \cos\alpha \tag{17}$$

Static optimization

However, the common and simplest approach is the static optimization, where the physiological character of the muscle is not considered:

$$a(t_k) = u_k \tag{18}$$

And

$$F^{MT}_{min} = 0 \tag{19}$$

$$F^{MT}_{max} = F^{M}_{0} \tag{20}$$

Multibody dynamics (MBD)

In this work, mixed coordinates (natural and relative) are used.

Matrix-R formulation is applied to set the equations of motion, and employed in both inverse- and forward-dynamics approaches.

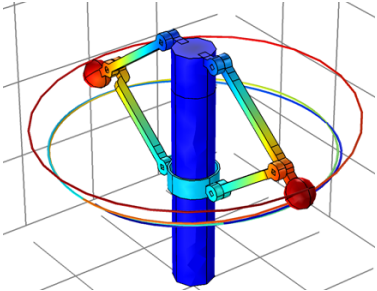

Matrix-R formulation

The constrained Lagrange equations constitute a system of index-3 differential-algebraic equations (DAE):

$$\mathbf{M}\ddot{\mathbf{q}} + \boldsymbol{\Phi}_{\mathbf{q}}{}^{\top}\boldsymbol{\lambda} = \mathbf{Q} \tag{21a}$$

$$\boldsymbol{\Phi} = \mathbf{0} \tag{21b}$$

- $\mathbf{M}$: mass matrix
- $\ddot{\mathbf{q}}$: accelerations vector of natural coordinates
- $\boldsymbol{\Phi}_{\mathbf{q}}$: Jacobian matrix of the constraints
- $\boldsymbol{\lambda}$: vector of Lagrange multipliers
- $\mathbf{Q}$: vector of external forces
- $\boldsymbol{\Phi}$: vector of constraint equations

Matrix-R formulation

The constrained Lagrange equations constitute a system of index-3 differential-algebraic equations (DAE):

$$\mathbf{M}\ddot{\mathbf{q}} + \boldsymbol{\Phi}_{\mathbf{q}}{}^{\top}\boldsymbol{\lambda} = \mathbf{Q} \tag{21a}$$

$$\boldsymbol{\Phi} = \mathbf{0} \tag{21b}$$

Matrix-R is a formulation in minimum number of coordinates obtained by applying a velocity transformation to the classical Lagrange's formulation of the first kind:

Velocity transformation:

$$\dot{\mathbf{q}} = \mathbf{R}\dot{\mathbf{z}} \tag{22}$$

$$\ddot{\mathbf{q}} = \dot{\mathbf{R}}\dot{\mathbf{z}} + \mathbf{R}\ddot{\mathbf{z}} \tag{23}$$

Matrix-R formulation

Matrix-R equations of motion:

$$\mathbf{R}^{\top}\mathbf{M}\mathbf{R}\ddot{\mathbf{z}} = \mathbf{R}^{\top}\left[\mathbf{Q} - \mathbf{M}\dot{\mathbf{R}}\dot{\mathbf{z}}\right] \tag{24}$$

- The number of equations is the same as the number of degrees of freedom of the model.
- $\mathbf{R}$ matrix and $\dot{\mathbf{R}}\dot{\mathbf{z}}$ vector require to be calculated at each time step by solving velocity and acceleration problems, respectively.
- This formulation is implemented in the in-house-developed library MBSLIM, programmed in FORTRAN language.

Data collection

Motion-force-EMG capture:

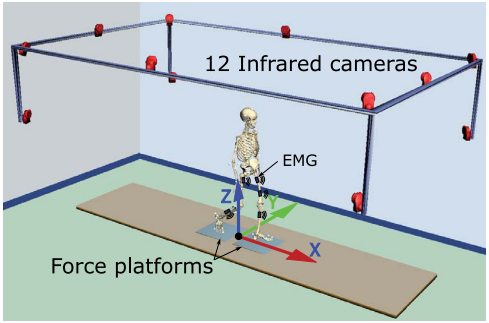

- 12 infrared cameras Natural Point, OptiTrack FLEX3:V100 sampling at 100 Hz,
- 2 force plates AMTI, AccuGait, sampling at 100 Hz,
- 16 wireless sensors of EMG telemetry system BTS FREEEMG sampling at 1 kHz,
- 1 portable gas analyzer Cortex MetaMax 3B.

Outline

The muscle force-sharing problem

The fundamental problem is that there are more muscles serving each degree of freedom of the system than those strictly necessary from the mechanical point of view, which implies that, in principle, an infinite number of recruitment patterns are acceptable.

- 43 muscles at the leg.
- 6 degrees of freedom considered as actuated by muscles at the leg.
- A specific strategy of muscle coordination is chosen by the CNS to perform a given motor task.

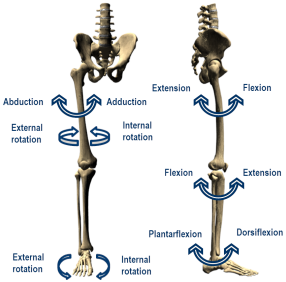

Inverse-dynamics based optimization

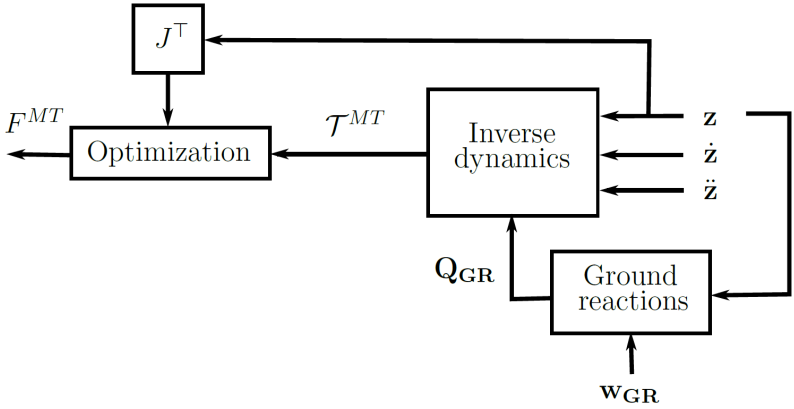

Optimization problem

In order to determine the muscle forces at each time-point, the inverse-dynamics based optimization problem can be formulated in general form as:

$$\begin{aligned} &\text{minimize or maximize} && C && (25)\\ &\text{subject to} && \mathcal{T}^{MT} = J^{\top} F^{MT} && (26)\\ & && F^{MT}_{i,min} < F^{MT} < F^{MT}_{i,max} \quad i = 1, ..., m && (27) \end{aligned}$$

- C is an objective function associated with decision variables. Expression of C depends on the muscle recruitment criteria used. In the literature, several muscle recruitment criteria have been suggested to represent the CNS behavior.
- The equality constraint obligates muscles to produce the corresponding intersegmental joint moments $\mathcal{T}^{MT}$.
- $F^{MT}_{i,min}$ and $F^{MT}_{i,max}$ are the instantaneous minimum and maximum allowed forces in muscle i, respectively.

Physiological approach (Phys.)

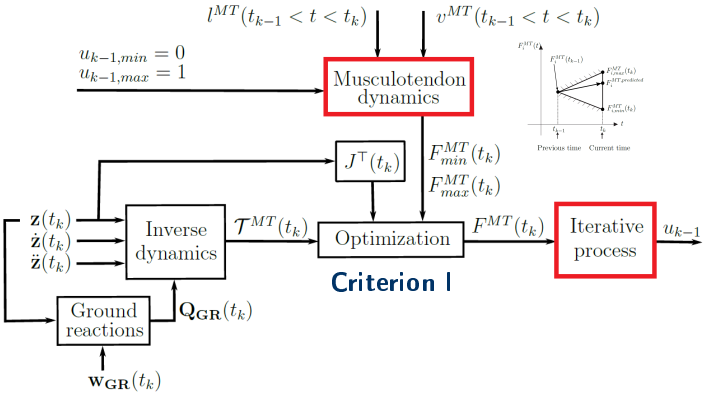

Physiological approach (Phys.)

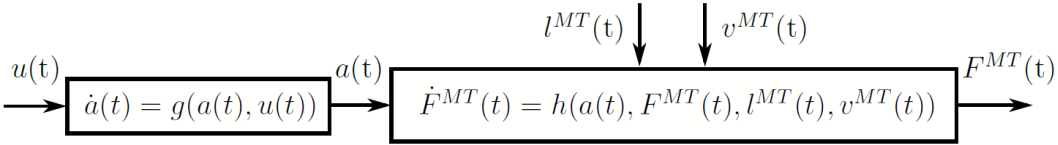

Phys. - *physiological approach with elastic tendon and activation dynamics.*

Phys. 2 - *physiological approach with rigid tendon and activation time response ignored.*

Phys. 3 - *physiological approach with rigid tendon and activation time response considered.*

Static optimization (SO)

Criterion I - *minimization of the sum of the squares of muscle forces*

$$\text{minimize} \quad \sum_{i=1}^{m} (F_i^{MT})^2 \tag{28}$$

Criterion II - *minimization of the sum of the squares of relative muscle forces*

$$\text{minimize} \quad \sum_{i=1}^{m} \left(\frac{F_i^{MT}}{F_{i,0}^{M}} \right)^2 \tag{29}$$

Criterion III - *minimization of the sum of the squares of muscle stresses*

$$\text{minimize} \quad \sum_{i=1}^{m} \left(\frac{F_i^{MT}}{PCSA_i} \right)^2 \tag{30}$$

Criterion IV - *minimization of the largest relative muscle force*

$$\text{minimize} \quad \max \left(\frac{F_i^{MT}}{F_{i,0}^{M}} \right), i = 1, ..., m \tag{31}$$

Results and experimental validation

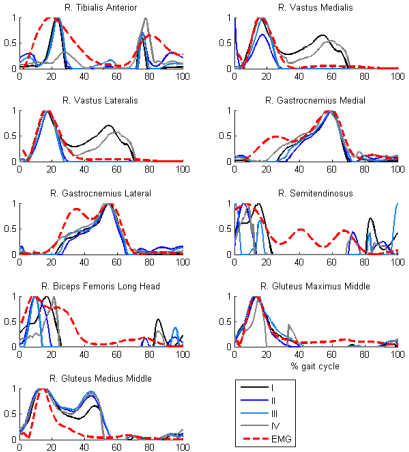

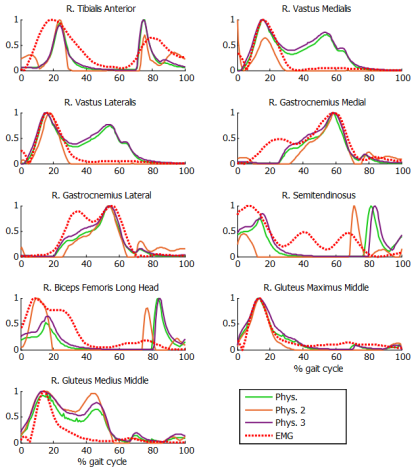

Results and experimental validation

	Mean correlation coefficient R values across subjects EMG vs. muscle activations						
	I	II	III	IV	Phys.	Phys. 2	Phys. 3
R. Tibialis Anterior	0,70	0,73	0,63	0,41	0,61	0,71	0,59
R. Vastus Medialis	0,69	0,67	0,83	0,45	0,69	0,69	0,69
R. Vastus Lateralis	0,73	0,71	0,87	0,53	0,71	0,73	0,71
R. Gastrocnemius Medial	0,80	0,65	0,77	0,75	0,80	0,61	0,82
R. Gastrocnemius Lateral	0,73	0,63	0,71	0,65	0,73	0,59	0,74
R. Semitendinosus	0,85	0,85	0,61	0,75	0,76	0,67	0,78
R. Biceps Femoris Long Head	0,81	0,85	0,75	0,72	0,69	0,74	0,74
R. Gluteus Maximus Middle	0,91	0,90	0,92	0,87	0,91	0,91	0,90
R. Gluteus Medius Middle	0,75	0,60	0,57	0,59	0,71	0,49	0,71
Mean	**0,77**	**0,73**	**0,74**	**0,64**	**0,74**	**0,68**	**0,74**
Computational time (sec)	2,2	49,3	26,5	31,9	351,4	2,0	2,6

Synergy optimization

B.J. Fregly

Rice University, Houston, Texas

M.S. Shourijeh

Research stay: March 1st - July 31st, 2018.

Muscle synergies

Analytical evidence that many muscles may share certain activity patterns.

Synergies take a high dimensional control space and reduce it to a low dimensional space.

Synergies were obtained by statistical analysis from surface EMG measurements.

$$\bar{a}_{syn} = \bar{A}_{syn} \times \bar{V}_{syn}. \quad (32)$$

For m muscles and s synergies during n time frames:

- $\bar{a}_{syn}[n \times s]$
- $\bar{A}_{syn}[n \times s]$
- $\bar{V}_{syn}[s \times m]$

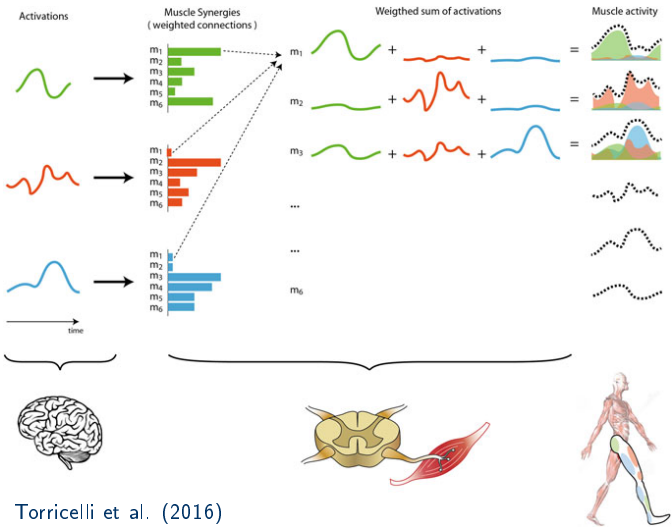

Torricelli et al. (2016)

Synergy optimization (SynO)

$$\text{minimize} \quad \beta \sum_{i=1}^{c} \sum_{j=1}^{n} \left[\frac{e_{kj,\mathcal{T}_i^{MT}}}{max(|\mathcal{T}_i^{MT}|)} \right]^2 + \gamma \sum_{k=1}^{m} \sum_{j=1}^{n} \bar{a}_{kj,syn}^2 \tag{33}$$

$$\text{subject to} \quad \sum_{j=1}^{s} \bar{V}_{ij,syn} = 1 \quad i = 1, ..., m \tag{34}$$

$$0 < N_{bj,syn} \quad b = 1, ..., p \quad and \quad j = 1, ..., s \tag{35}$$

$$0 < \bar{V}_{ij,syn} \quad i = 1, ..., m \quad and \quad j = 1, ..., s \tag{36}$$

Shourijeh MS., Fregly BJ. Muscle synergies modify static optimization estimates of joint stiffness during walking. J. Biomech. Eng. 2019 July.

Synergy optimization (SynO)

$$\text{minimize} \quad \beta \sum_{i=1}^{c} \sum_{j=1}^{n} \left[\frac{e_{kj,\mathcal{T}_i^{MT}}}{max(|\mathcal{T}_i^{MT}|)} \right]^2 + \gamma \sum_{k=1}^{m} \sum_{j=1}^{n} \bar{a}_{kj,syn}^2 \tag{33}$$

$$\text{subject to} \quad \sum_{j=1}^{s} \bar{V}_{ij,syn} = 1 \quad i = 1, ..., m \tag{34}$$

$$0 < N_{bj,syn} \quad b = 1, ..., p \quad and \quad j = 1, ..., s \tag{35}$$

$$0 < \bar{V}_{ij,syn} \quad i = 1, ..., m \quad and \quad j = 1, ..., s \tag{36}$$

Synergy activations are represented by b-spline curves with p nodal points.

The problems remain under-determined since neighboring time frames are not independent from one another.

For m muscles and s synergies during n time frames:

- $s * (p + m)$ design variables.

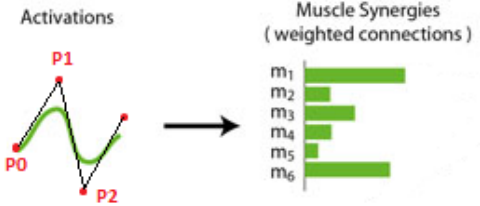

Synergy optimization (SynO)

$$\text{minimize} \quad \beta \sum_{i=1}^{c} \sum_{j=1}^{n} \left[\frac{e_{kj,\mathcal{T}_i^{MT}}}{max(|\mathcal{T}_i^{MT}|)} \right]^2 + \gamma \sum_{k=1}^{m} \sum_{j=1}^{n} \bar{a}_{kj,syn}^2 \tag{33}$$

$$\text{subject to} \quad \sum_{j=1}^{s} \bar{V}_{ij,syn} = 1 \quad i = 1, ..., m \tag{34}$$

$$0 < N_{bj,syn} \quad b = 1, ..., p \quad and \quad j = 1, ..., s \tag{35}$$

$$0 < \bar{V}_{ij,syn} \quad i = 1, ..., m \quad and \quad j = 1, ..., s \tag{36}$$

- B-spline nodes (N) of the synergy activation and synergy vector weights greater than zero.
- Sum of weights within each synergy vector equal to one, which makes the synergy construction unique.
- $e_{kj,\mathcal{T}_i^{MT}} = \mathcal{T}_{i,j}^{MT} - \mathcal{T}_{i,j}^{ID}$, the inverse-dynamics joint moment errors.

Extraction of synergies from static optimization (SO-NMF)

- SynO:
  - Complex to implement because of the b-spline curves.
  - Resolution of the optimization problem very slow because of the high number of design variables.
- SO:
  - Good correlations with EMG measurements.
  - Easy to implement and fast calculation.
  - All the muscles of the model are considered.

Extraction of synergies from static optimization (SO-NMF)

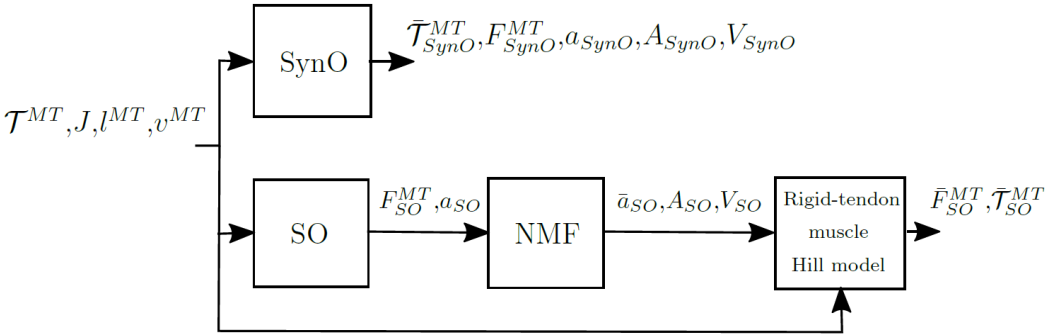

Results and experimental validation

Mean R^2 values across subjects for joint moment matching

	2 synergies		3 synergies		4 synergies		5 synergies		6 synergies		SO
	SynO	SO-NMF	SynO	SO-NMF	SynO	SO-NMF	SynO	SO-NMF	SynO	SO-NMF	
Hip Abd/Add	0,93	0,76	0,97	0,85	0,99	0,94	0,99	0,97	1,00	0,97	1,00
Hip Flex/Ext	0,94	0,82	0,98	0,95	0,99	0,96	1,00	0,98	1,00	0,98	1,00
Hip Int/Ext rot.	0,94	0,32	0,98	0,37	0,99	0,40	1,00	0,56	1,00	0,54	1,00
Knee Flex/Ext	0,93	0,37	0,97	0,57	0,98	0,87	0,99	0,94	1,00	0,94	1,00
Ankle Int/Ext rot.	0,76	0,55	0,92	0,57	0,98	0,74	1,00	0,83	1,00	0,85	1,00
Ankle Flex/Ext	0,92	0,78	0,96	0,83	0,98	0,87	0,99	0,89	1,00	0,92	1,00
Mean	0,90	0,60	0,96	0,69	0,99	0,80	1,00	0,86	1,00	0,87	1,00

- SO's equality constraints force the muscles to produce the inverse-dynamics joint moments.
  - SO presents perfect correlations with the experimental inverse-dynamics joint moments.
- SynO minimizes the inverse-dynamics joint moments error while SO-NMF doesn't have any restrictions.
  - SO-NMF matches poorly the experimental inverse-dynamics joint moments.
  - SynO presents good or very good (>95%) correlations according to the number of synergy.

Results and experimental validation

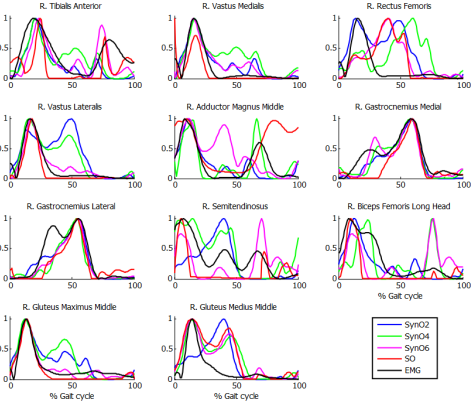

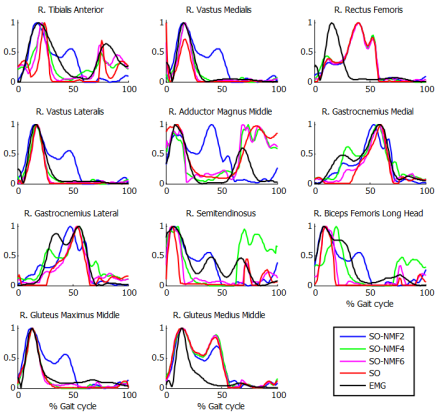

Results

	Mean correlation coefficient R values across subjects EMG vs. Muscle activations										
	2 Synergies		3 Synergies		4 Synergies		5 Synergies		6 Synergies		SO
	SynO	SO-NMF	SynO	SO-NMF	SynO	SO-NMF	SynO	SO-NMF	SynO	SO-NMF	
R. Tibialis Anterior	0,58	0,52	0,59	0,75	0,56	0,75	0,56	0,74	0,69	0,76	0,69
R. Vastus Medialis	0,84	0,74	0,61	0,84	0,68	0,74	0,68	0,75	0,73	0,76	0,71
R. Vastus Lateralis	0,72	0,74	0,75	0,82	0,65	0,80	0,54	0,78	0,73	0,79	0,74
R. Adductor Magnus Middle	0,48	0,54	0,43	0,71	0,52	0,51	0,57	0,56	0,57	0,56	0,52
R. Gastrocnemius Medial	0,72	0,80	0,87	0,71	0,77	0,67	0,70	0,69	0,75	0,67	0,60
R. Gastrocnemius Lateral	0,57	0,72	0,76	0,77	0,67	0,66	0,70	0,70	0,64	0,71	0,57
R. Semitendinosus	0,36	0,73	0,58	0,89	0,53	0,66	0,66	0,67	0,50	0,60	0,57
R. Biceps Femoris Long Head	0,72	0,69	0,57	0,85	0,51	0,79	0,50	0,80	0,54	0,86	0,84
R. Gluteus Maximus Middle	0,74	0,71	0,71	0,86	0,71	0,90	0,84	0,92	0,87	0,92	0,91
R. Gluteus Medius Middle	0,25	0,39	0,45	0,41	0,36	0,40	0,48	0,42	0,38	0,43	0,44
Mean	**0,60**	**0,66**	**0,63**	**0,76**	**0,60**	**0,69**	**0,62**	**0,70**	**0,64**	**0,71**	**0,66**
Computational time (sec)	80	4	115	4	196	4	317	4	587	4	2

- No significant differences are observed for different numbers of synergies.
- Strangely, the reconstructed activations from SO-NMF match EMG better than do the original activations from SO.
- The CNS could control one leg during gait using only three synergies.
- Synergy structure and reduced dimensional control space could be useful for some applications.

Forward-dynamics based optimization

Computed Muscle Control (CMC)

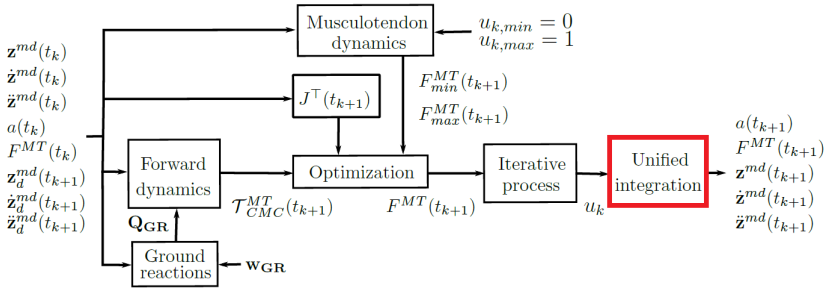

Darryl G. Thelen, Frank C. Anderson, and Scott L. Delp. Generating dynamic simulations of movement using computed muscle control. Journal of Biomechanics, 36(3):321-328, 2003.

Forward-dynamics based optimization

Co-simulation algorithm (CS)

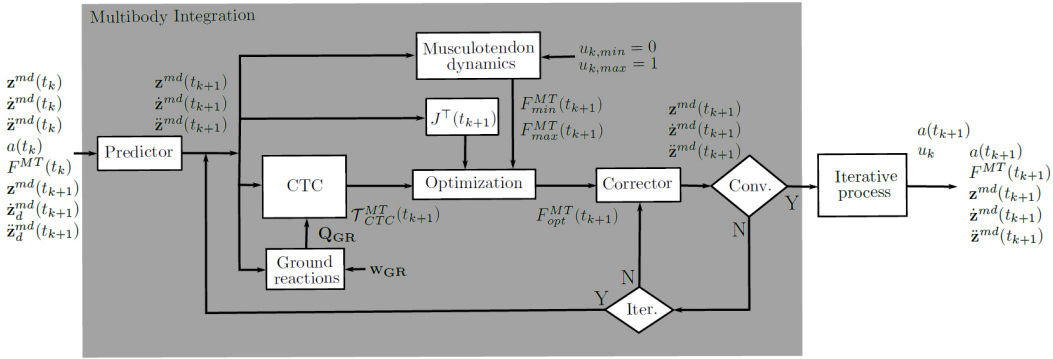

F. Michaud, U. Lugris, J. Cuadrado. A Co-integration Approach for the Forwarddynamics Based Solution of the Muscle Recruitment Problem. 7o Congresso Nacional de Biomecanica. Guimaraes, Portugal, 2017-02.
(**Best Theoretical Paper Award**)

Forward-dynamics based optimization

Computed Muscle Control (CMC)

$$\ddot{\mathbf{z}}^{md}_{CMC}(t_{k+1}) = \ddot{\mathbf{z}}^{md}_{d}(t_{k+1}) + k_v\dot{\varepsilon}_k + k_p\varepsilon_k \qquad (37)$$

- Set of controller accelerations is calculated from errors at the actual time step.
- The whole system of equations is integrated one step forward, in a unified scheme.
- A single muscle optimization is carried out at every time step.

Co-simulation algorithm (CS)

$$\ddot{\mathbf{z}}^{md}_{CTC}(t_{k+1}) = \ddot{\mathbf{z}}^{md}_{d}(t_{k+1}) + k_v\dot{\varepsilon}_{k+1} + k_p\varepsilon_{k+1} \qquad (38)$$

- Set of controller accelerations is calculated from predicted errors at the next time step.
- Multibody and muscular dynamic equations are integrated separately.
  - Allow to use existing multibody codes by simulating the multibody equations and the muscular dynamics in a different framework.
- An implicit integrator, in a predictor-corrector scheme, is used to integrate the multibody equations.
  - Simplified approach: only one optimization at the first iteration, using the predictor estimate.

Results and experimental validation

Simple pendulum

- Simple pendulum actuated by two muscles.
- To play the role of the experimentally acquired motion in biomechanical examples, a predefined history of the angle is imposed.
- 3 methods compared: CMC, co-simulation standard (CSS), and co-simulation approximated (CSA).
- Integration carried out with trapezoidal rule.

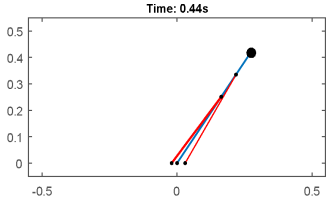

t(s)	θ (º)
0	180
1/3	180-60
2/3	180+60
1	180

Results and experimental validation

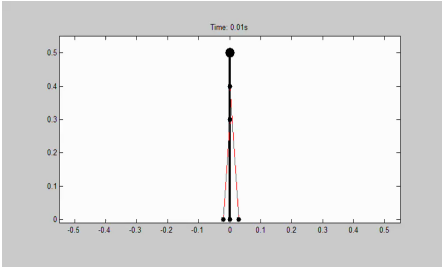

Method	CPU time (s)	RMS error (deg)
CMC	8.25	0.0025
CSS	23.66	0.0186
CSA	7.85	0.1146

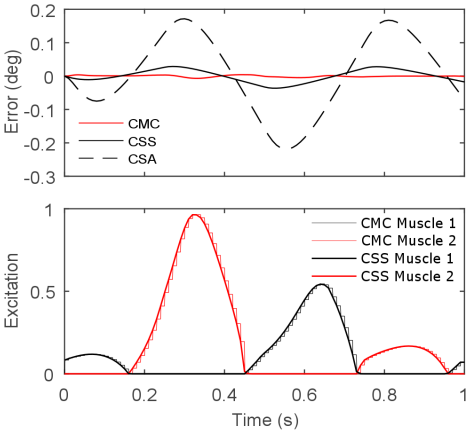

Results and experimental validation

Because the optimization method in the co-simulation standard algorithm does not require to be physiological, all the criteria studied before for inverse dynamics can be used and compared using forward dynamics and this approach.

	Mean correlation coefficient R values across subjects EMG vs. muscle activations					
	I	II	III	IV	Phys.	Phys. 3
R. Tibialis Anterior	0,74	0,73	0,72	0,51	0,69	0,62
R. Vastus Lateralis	0,73	0,74	0,88	0,56	0,85	0,65
R. Adductor Magnus Middle	0,58	0,48	0,39	0,55	0,65	0,61
R. Gastrocnemius Medial	0,80	0,66	0,76	0,75	0,64	0,66
R. Gastrocnemius Lateral	0,72	0,62	0,62	0,67	0,65	0,59
R. Semitendinosus	0,76	0,79	0,79	0,75	0,64	0,67
R. Biceps Femoris Long Head	0,77	0,81	0,84	0,70	0,21	0,56
R. Gluteus Maximus Middle	0,92	0,91	0,93	0,88	0,93	0,93
R. Gluteus Medius Middle	0,75	0,58	0,61	0,59	0,63	0,72
Mean	**0,75**	**0,70**	**0,73**	**0,66**	**0,66**	**0,67**
Computational time (sec)	16,35	360,07	175,77	247,75	1828,71	27,32

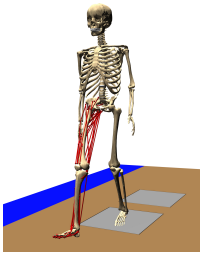

- No significant differences are observed with respect to the results obtained through the inverse-dynamics approach.
- Iterative process makes the computation slower.

Outline

Muscle energy expenditure

- 2 methods are implemented in this work to calculate the energetic cost of healthy subjects in normal gait and of SCI subjects in crutch gait:
  - Umberger and Bhargava.
- Muscle activation, length, velocity and muscular force are obtained by physiological static optimization method and they are used as input.
- Both models are based on the first law of thermodynamics.

$$\dot{E} = \dot{H} + \dot{W} \tag{39}$$

Muscle energy expenditure methods

Umberger

$$\dot{E} = \dot{h}_A + \dot{h}_M + \dot{h}_{SL} + \dot{w}_{CE} \quad (40)$$

- $\dot{h}_A$: activation heat rate.
- $\dot{h}_M$: maintenance heat rate.
- $\dot{h}_{SL}$: shortening and lengthening heat rate.
- $\dot{w}_{CE}$: mechanical work rate.

Muscle energy expenditure methods

Umberger

$$\dot{E} = \dot{h}_A + \dot{h}_M + \dot{h}_{SL} + \dot{w}_{CE} \quad (40)$$

- $\dot{h}_A$: activation heat rate.
- $\dot{h}_M$: maintenance heat rate.
- $\dot{h}_{SL}$: shortening and lengthening heat rate.
- $\dot{w}_{CE}$: mechanical work rate.

Bhargava

$$\dot{E}^* = \dot{h}_A^* + \dot{h}_M^* + \dot{h}_{SL}^* + \dot{w}_{CE}^* + \dot{h}_B \quad (41)$$

- $\dot{h}_B = 0.0225$: basal metabolic rate.

Muscle energy expenditure methods

Umberger

$$\dot{E} = \dot{h}_A + \dot{h}_M + \dot{h}_{SL} + \dot{w}_{CE} \quad (40)$$

- $\dot{h}_A$: activation heat rate.
- $\dot{h}_M$: maintenance heat rate.
- $\dot{h}_{SL}$: shortening and lengthening heat rate.
- $\dot{w}_{CE}$: mechanical work rate.

Bhargava

$$\dot{E}^* = \dot{h}_A^* + \dot{h}_M^* + \dot{h}_{SL}^* + \dot{w}_{CE}^* + \dot{h}_B \quad (41)$$

- $\dot{h}_B = 0.0225$: basal metabolic rate.

Total energy expenditure during a gait cycle

$$E_{met} = \left(\sum_{i=1}^{n} \left(\frac{\int_{t=0}^{t_{cycle}} \dot{E}_i(t) \times m_i \, dt}{\Delta t_{cycle}} \right) + k_b \times m_{residual} \right) / m_{subject} \quad (42)$$

- $k_b = 1.2 \ W.kg^{-1}$: whole-body basal metabolic rate.

Results and experimental validation

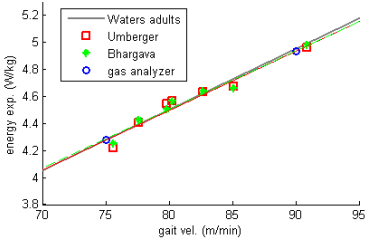

- Calibration of y-intercept (k_b):
  - Umberger: $+0.12\ W.kg^{-1}$.
  - Bhargava: $+1.9\ W.kg^{-1}$.
- The slopes (energy cost vs. gait speed) obtained with both methods were coincident and agreed with those from literature and experimental values, which is the essential point to compare two activities performed by the same subject and using the same method.

- 21 complete gait cycles of a healthy subject recorded at 7 different speeds.
- 2 5-minute tests with portable gas analyzer at free selected speed and fast speed.

Outline

SCI subjects

- The extent of paralysis depends on the location of the wound in the spine and its severity.
- The level of the injury is not enough to determine the associated damage.
- American Spinal Injury Association (ASIA) published the LEMS:

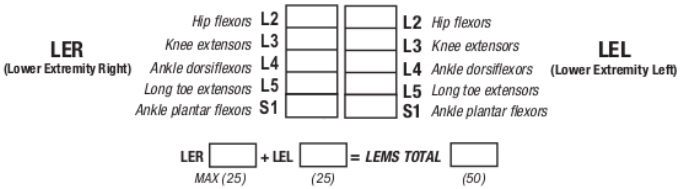

Lower Extremity Motor Score (LEMS)

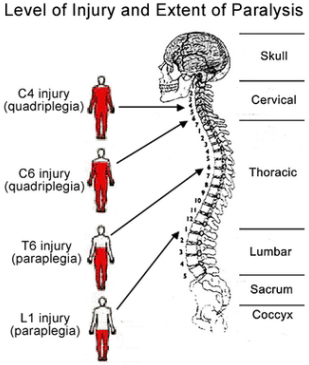

Adaptation process

Subject evaluation

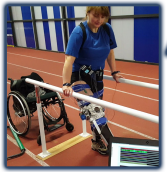

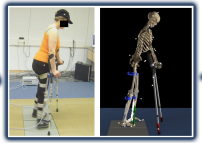

Pre-analysis

Customized active KAFO

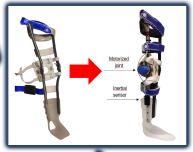

Parallel bars training

Crutch gait

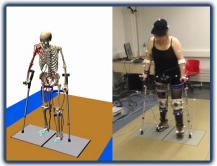

Gait analysis at musculoskeletal level to estimate the joint reactions and the energetic cost to assess the suitability of the orthotic device for the subject.

Bilateral SCI subject

Subject characteristics

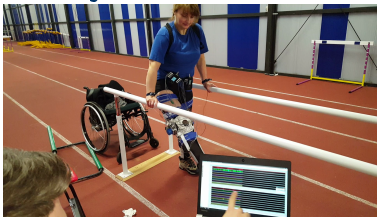

- Adult female of 45-year-old.
- Mass 65 kg and height 1.52 m.
- Spinal cord injury at T11:
  - Normal motion of the upper extremities and trunk.
  - Partially limited hip actuation.
  - **LEMS: 10/50**.

Bilateral SCI subject

Subject characteristics

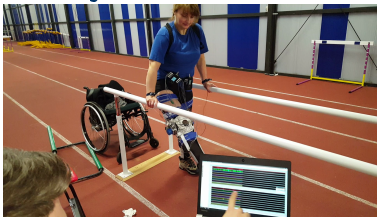

- Adult female of 45-year-old.
- Mass 65 kg and height 1.52 m.
- Spinal cord injury at T11:
  - Normal motion of the upper extremities and trunk.
  - Partially limited hip actuation.
  - **LEMS: 10/50**.

Personalized musculoskeletal model

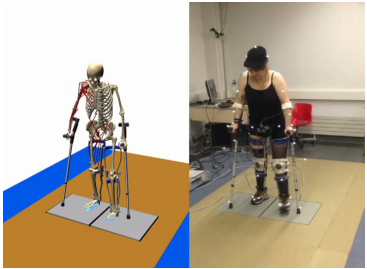

- 53 muscles at the right side:
  - 21 at the right hip.
  - 6 at the trunk.
  - 15 at the right shoulder.
  - 11 at the right elbow.

Bilateral SCI subject

Results and experimental validation (passive orthoses)

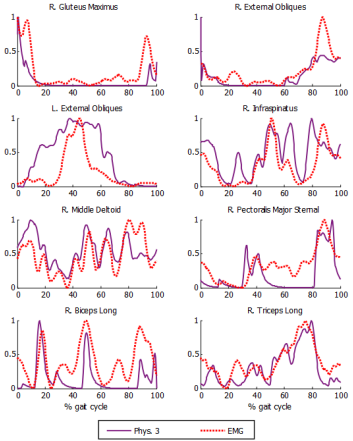

	Correlation coefficient R EMG vs. muscle activations
R. Gluteus Maximus Posterior	0,68
R. External Obliques	0,89
L. External Obliques	0,76
R. Infraspinatus	0,63
R. Middle Deltoid	0,57
R. Pectoralis Major Sternal	0,75
R. Biceps Long	0,50
R. Triceps Long	0,86
Mean	**0,70**

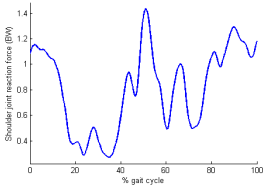

Right shoulder joint reaction force

Bilateral SCI subject

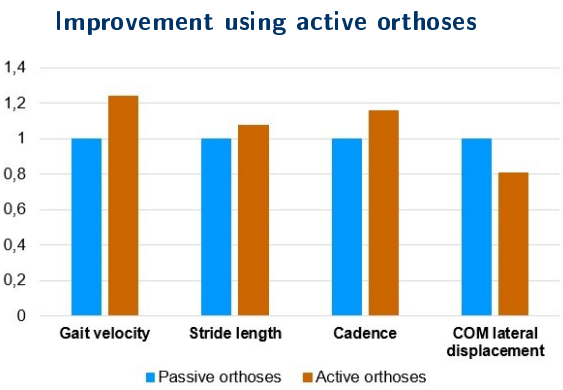

Portable motion capture system

Unilateral SCI subject

Subject characteristics

- Adult male of 49-year-old.
- Mass 82 kg and height 1.85 m.
- Spinal cord injury:
  - Normal motion of the upper extremities, trunk and hips.
  - Knee actuation only at the right leg.
  - **LEMS: 13/50**.

Unilateral SCI subject

Subject characteristics

- Adult male of 49-year-old.
- Mass 82 kg and height 1.85 m.
- Spinal cord injury:
  - Normal motion of the upper extremities, trunk and hips.
  - Knee actuation only at the right leg.
  - **LEMS: 13/50**.

Personalized musculoskeletal model

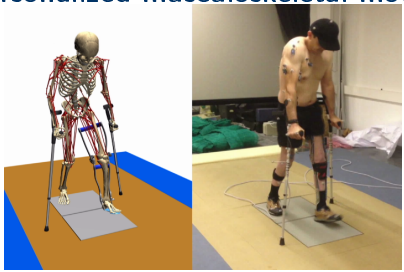

- 112 muscles for the whole body:
  - 28 at the right hip, 21 at the left hip.
  - 6 at the trunk.
  - 15 at each shoulder.
  - 11 at each elbow.

Unilateral SCI subject

Results and experimental validation

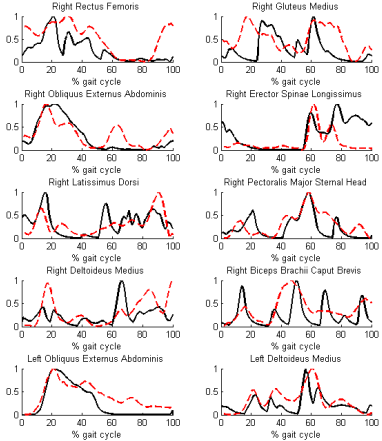

- Mean coefficient correlation R of 56%.
- Validates the personalized musculoskeletal model used.
- Validates the inputs provided to the energetic cost calculations.

Unilateral SCI subject

Improvement using active orthoses

		passive KAFO	active KAFO (locked knee)	active KAFO (moving knee)
Gait velocity (m/min)		33	33	33
Vertical COM displacement (cm)		3.47	3.79	4.11
Mediolateral COM displacement (cm)		13.48	13.42	11.54
Step length (cm)	Right	0.45	0.52	0.58
	Left	0.66	0.62	0.58
Left circumduction (cm)		11.52	9.10	7.25
Range pelvic rotations in frontal plane (°)		[-4.81; 19.18]	[-4.56; 16.93]	[-4.86; 15.23]
Range pelvic rotations in transverse plane (°)		[-28.74; 42.87]	[-28.32; 37.93]	[-24.36; 31.83]
Energy cost(W/kg)	Umberger	3.49	3.56	3.28
	Bhargava	3.11	3.13	3.02

- Symmetry in the step lengths, reduced circumduction and reduced pelvic rotation.
- Motor actuation reduced significantly (almost 8% for Umberger and 3.5% for Bhargava) the estimated energy consumption despite the short period of training with the device.

Outline

Conclusions

- Inverse-dynamics based methods:
  - Four static and three physiological inverse-dynamics based optimization approaches were compared first, and showed similar results.
  - Higher complexity of the method does not guarantee better results.
  - Physiological inverse-dynamics approach was hard to implement and presented the longest computational time (the simplified form was 100 times faster).
  - Same conclusions can be drawn for the synergy optimization approach studied in this thesis.
  - SynO approach can extract muscular synergies and offer a reasonable prediction of muscular activations and matching of the joint torques for the full leg.
- Forward-dynamics based methods:
  - Co-simulation algorithm approach proposed allowed to use existing multibody codes by simulating the multibody equations and the muscular dynamics in a different framework.
  - Standard approach, CSS, was slowest than the reference method CMC due to its numerous optimizations and integrations.
  - Approximated approach showed better computational performance than CMC but its accuracy was affected.
  - Comparison using co-simulation standard algorithm and several optimization criteria presented the same conclusions as for the inverse-dynamics analysis: the simplest criterion was the most accurate.

Conclusions

- Muscle energy expenditure:
  - Results of the inverse-dynamics based approach are required as inputs for the muscular variables.
  - The slopes (energy cost vs. gait speed) obtained with both methods were coincident and agreed with those from literature and experimental values, which is the essential point to compare two activities performed by the same subject and using the same method.
- Applications to SCI subjects:
  - Each SCI subject required a customized musculoskeletal model corresponding to his injury.
  - The first subject showed significant improvements thanks to the motor actuation in both knees.
  - The second subject improved his gait pattern and reduced his energy consumption by using the actuated assistive device.
  - Crutch-orthosis-assisted gait is challenging for SCI subjects: low speed, high demand of muscular activity, and risk of suffering upper limb injuries, especially at shoulders.
  - Musculoskeletal models can help to design and evaluate gait-assistive devices or medical treatments.

Future work

- Comparison between the results obtained from the motion-force-EMG capture of the five healthy subjects by the in-house developed methods and the reference software OpenSim.
  - For the kinematics, joint torques and estimated muscular activations.
- Estimation of the energy expenditure by using the rigid tendon model.
- Continuation of the study for a longer period, with more SCI subjects, to see the evolution of joint reactions and energetic cost as users become more acquainted with the new devices.

Works derived from this thesis

- Published and accepted book paper and journal papers
  - J. Cuadrado, U. Lugrís, F. Mouzo, F. Michaud. Musculo-skeletal modeling and analysis for low-cost active orthosis customization and SCI patient adaptation. IUTAM Symposium on Intelligent Multibody Systems - Dynamics, Control, Simulation, ed. by E. Zahariev and J. Cuadrado, Springer, 2019.
  - F. Michaud, F. Mouzo, U. Lugrís, J. Cuadrado. Energy expenditure estimation during crutch-orthosis-assisted gait of a spinal-cord-injured subject. Frontiers in Neurorobotics, vol. 13, article 55, 11 pages, 2019.
  - F. Mouzo, F. Michaud, U. Lugrís, J. Cuadrado. Leg-orthosis contact force estimation from gait analysis. Mechanism and Machine Theory, 2020.
- Submitted journal papers (under review)
  - F. Michaud, U. Lugrís, J. Cuadrado, A. Kecskemethy. A procedure to define customized musculoskeletal models for the analysis of the crutch-orthosis-assisted gait of SCI subjects. J. of Biomechanical Engineering.
  - F. Michaud, M.S. Shourijeh, B.J. Fregly, J. Cuadrado. Do muscle synergies improve optimization prediction of muscle activations during gait? Frontiers In Computational Neuroscience.

Conference communications

- U. Lugris, J. Carlin, F. Michaud, J. Cuadrado. Joint Efforts Calculation in the Gait of Incomplete Spinal Cord Injured Subjects. 2nd Joint Int. Conference on Multibody System Dynamics (IMSD). Stuttgart, Germany, 2012-05.
- J. Cuadrado, U. Lugris, F. Michaud, F. Mouzo. Role of Multibody Dynamics Based Simulation in Human, Robotic and Hybrid Locomotion Benchmarking. Workshop on Benchmarking Bipedal Locomotion, 2014 IEEE-RAS Int. Conference on Humanoid Robots. Madrid, Spain, 2014-11.
- F. Michaud, U. Lugris, Y. Ou, J. Cuadrado, A. Kecskemethy. Influence of Muscle Recruitment Criteria on Joint Reaction Forces During Human Gait. ECCOMAS Thematic Conference on Multibody Dynamics 2015. Barcelona, Spain, 2015-06.
- F. Michaud, U. Lugris, Y. Ou, J. Cuadrado, A. Kecskemethy. Comparison of Forward-dynamics Approaches to Estimate Muscular Forces in Human Gait. 4th Joint Int. Conference on Multibody System Dynamics (IMSD 2016). Montreal, Canada, 2016-05.
- F. Michaud, U. Lugris, J. Cuadrado. A Co-integration Approach for the Forward-dynamics Based Solution of the Muscle Recruitment Problem (Premio al mejor trabajo teórico). 7º Congresso Nacional de Biomecânica. Guimaraes, Portugal, 2017-02.
- F. Michaud, U. Lugris, Y. Ou, J. Cuadrado, A. Kecskemethy. Optimization Methods for Identifying Muscle Forces in a Spinal-cord-injured Subject during Crutch-assisted Gait. 8th ECCOMAS Thematic Conference on Multibody Dynamics. Prague, Czech Republic, 2017-06.
- J. Cuadrado, U. Lugris, F. Mouzo, F. Michaud. Strain Measurements in Active Orthoses for Multibody Model Validation and Control Robustness Improvement. IUTAM Symposium on Intelligent Multibody Systems: Dynamics, Control, Simulation. Sozopol, Bulgaria, 2017-09.
- U. Lugris, R. Vilela, E. Sanjurjo, F. Mouzo, F. Michaud. Implementation of an Extended Kalman Filter for Robust Real-time Motion Capture Using IR Cameras and Optical Markers. IUTAM Symposium on Intelligent Multibody Systems: Dynamics, Control, Simulation. Sozopol, Bulgaria, 2017-09.
- F. Michaud, U. Lugris, J. Castro, J. Cuadrado. Estimation of Muscle Energy Expenditure in a Spinal-cord-injured Subject during Crutch-assisted Gait. 5th Joint Int. Conference on Multibody System Dynamics (IMSD 2018). Lisbon, Portugal, 2018-06.
- U. Lugris, R. Vilela, E. Sanjurjo, F. Mouzo and F. Michaud. Implementation of an Extended Kalman Filter for Optical Motion Capture with Real-time 3D Visualization. 5th Joint Int. Conference on Multibody System Dynamics (IMSD 2018). Lisbon, Portugal, 2018-06.
- J. Cuadrado, U. Lugris, F. Mouzo and F. Michaud. Skeletal Multibody Model for Leg-Orthosis Contact Force Estimation in SCI Subjects. 12th Int. Congress on Mechanics, HSTAM 2019. Thessaloniki, Greece, 2019-09.

Neuromusculoskeletal human multibody models for the gait of healthy and spinal-cord-injured subjects

Thank you for your attention!

EMG treatment

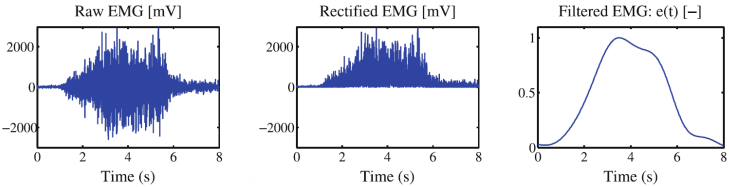

EMG signal :

- Rectified.
- Filtered by singular spectrum analysis (SSA) with a window length of 250 (Romero et al. 2015) (equivalent to the common forward and reverse low-pass 5th order Butterworth filter with a cut-off frequency of 15 Hz).
- Normalized with respect to its maximal value.

(Raison et al. 2011)

Optimization protocol

An optimization problem is the problem of finding the best solution from all feasible solutions by minimizing the objective function. Finding the global minima of a function is really difficult because of the many local minima. In order to get the best possible results, the following protocol has been used for all the optimization problems of this work:

- Initial time step:
  - 5 global optimizations are run using Matlab's *ga* genetic optimization algorithm with a population size of 50.
  - The solution with the lowest objective function of the 5 values is chosen as initial guess for Matlab's *fmincon* function.
- Next time steps:
  - Solution of the previous time step is used as initial guess for *fmincon*.

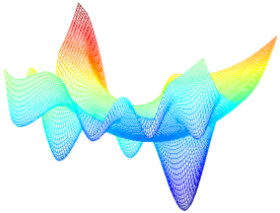

Calculation of the Jacobian of muscle moment arms

$$\vec{F}^{MT} = F^{MT}\,\vec{u}^{MT} \tag{43}$$

$$\vec{u}^{MT} = \frac{\vec{r}_{Oe} - \vec{r}_{Ie}}{\|\vec{r}_{Oe} - \vec{r}_{Ie}\|} \tag{44}$$

$$\mathcal{T}^{MT} = J^{\top} F^{MT} \tag{45}$$

$$\vec{d} = \vec{u}^{MT} \wedge \vec{r} = [d_x\, d_y\, d_z]^{\top} \tag{46}$$

$$J^{\top} = [\vec{d}_1 \ldots \vec{d}_i \ldots \vec{d}_m] \tag{47}$$

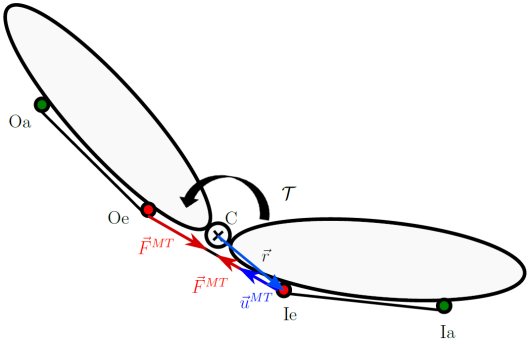

Muscular parameters scaling

- l_S^T
- l_0^M

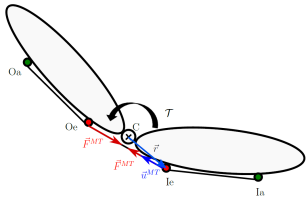

$$l^{MT} = \sum_{i=1}^{n-1} s_i \tag{48}$$

$$fact_{s,i} = \frac{l_{i,ref}^{MT}}{l_{i,scal}^{MT}} \tag{49}$$

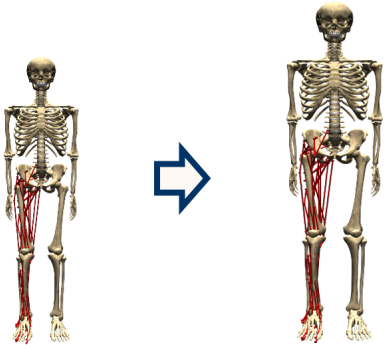

Reference model	Scaled model
$l_{i,ref}^{MT}$	$l_{i,scal}^{MT}$

Muscular parameters scaling

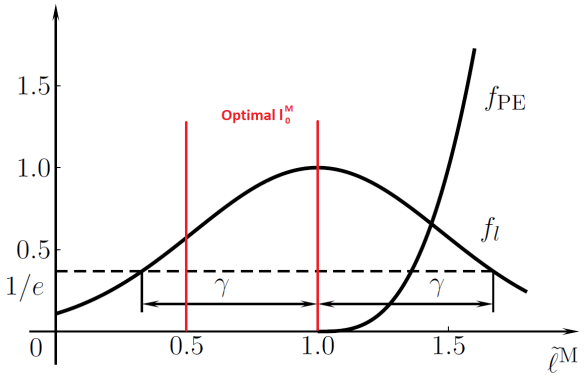

$$l^M_{0,opti} = max(l^{MT}) - l^T_{S,scaled} \quad (50)$$

Muscle geometry

```
<Thelen2003Muscle name="glut_max1_r">
    <!--Flag indicating whether the force is disabled or not. Disab
    <isDisabled>false</isDisabled>
    <!--Minimum allowed value for control signal. Used primarily wh
    <min_control>0</min_control>
    <!--Maximum allowed value for control signal. Used primarily wh
    <max_control>1</max_control>
    <!--The set of points defining the path of the muscle.-->
    <GeometryPath>
        <PathPointSet>
            <objects>
                <PathPoint name="glut_max1_r-P1">
                    <location> -0.1195 0.0612 0.07</location>
                    <body>pelvis</body>
                </PathPoint>
                <PathPoint name="glut_max1_r-P2">
                    <location> -0.1291 0.0012 0.0886</location>
                    <body>pelvis</body>
                </PathPoint>
                <PathPoint name="glut_max1_r-P3">
                    <location> -0.0457 -0.0248 0.0392</location>
                    <body>femur_r</body>
                </PathPoint>
                <PathPoint name="glut_max1_r-P4">
                    <location> -0.0277 -0.0566 0.047</location>
                    <body>femur_r</body>
                </PathPoint>
            </objects>
            <groups />
        </PathPointSet>
```

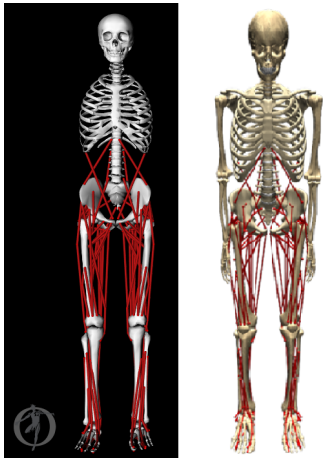

Model: Gait2392 (43/leg + 6 at trunk)

Umberger

- Activation and maintenance heat rate

$$\dot{h}_A + \dot{h}_M = \dot{h}_{AM} = 1.28 \times \%FT + 25 \tag{51}$$

- Shortening and lengthening heat rate

$$\dot{h}_{SL} = \begin{cases} \alpha_{S(ST)}\tilde{v}^M(1 - \%FT/100) - \alpha_{S(FT)}\tilde{v}^M(\%FT/100) & \text{if} \quad v^M \leq 0, \\ \alpha_L \tilde{v}^M & \text{if} \quad v^M > 0, \end{cases} \tag{52}$$

- Mechanical work rate

$$\dot{w}_{CE} = -(F_{CE}^M v^M)/m \tag{53}$$

- Muscle mass (kg)

$$m = PCSA\rho_m l_0^M \tag{54}$$

$\rho_m = 1059.7\ kg.m^{-3}$, the mammalian muscle density

Bhargava

- Activation and maintenance heat rate

$$\dot{h}_A = \phi f_{FT} \dot{A}_{FT} u_{FT}(t) + \phi f_{ST} \dot{A}_{ST} u_{ST}(t) \tag{55}$$

$$\dot{h}_M = L(\tilde{l}^M) f_{FT} \dot{M}_{FT} u_{FT}(t) + L(\tilde{l}^M) f_{ST} \dot{M}_{ST} u_{ST}(t) \tag{56}$$

- Shortening and lengthening heat rate

$$\dot{h}_{SL} = -\alpha_S v^M \tag{57}$$

- Mechanical work rate

$$\dot{w}_{CE} = -(F_{CE}^M v^M)/m \tag{58}$$

Inverse dynamics

Matrix-R equations of motion:

$$\mathbf{R}^{\top}\mathbf{M}\mathbf{R}\ddot{\mathbf{z}} = \mathbf{R}^{\top}\left[\mathbf{Q} - \mathbf{M}\dot{\mathbf{R}}\dot{\mathbf{z}}\right] \tag{59}$$

$$\bar{\mathbf{M}}\ddot{\mathbf{z}} = \mathbf{Q_m} + \mathbf{Q_c} \tag{60}$$

$$\mathbf{Q_m} = \bar{\mathbf{M}}\ddot{\mathbf{z}} - \mathbf{Q_c} \tag{61}$$

- $\mathbf{Q_m}$: vector of generalized motor forces.
- $\mathbf{Q_c}$: vector grouping all the remaining generalized forces (centrifugal and Coriolis forces).

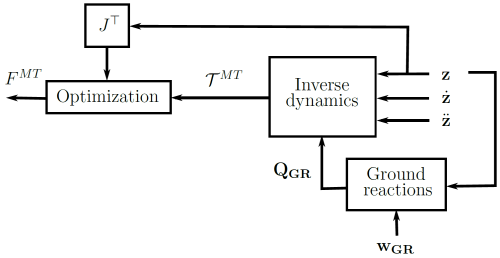

Forward dynamics: Computed Torque Control

Matrix-R equations of motion:

$$\mathbf{R}^\top \mathbf{M}\mathbf{R}\ddot{\mathbf{z}} = \mathbf{R}^\top \left[\mathbf{Q} - \mathbf{M}\dot{\mathbf{R}}\dot{\mathbf{z}}\right] \tag{62}$$

$$\bar{\mathbf{M}}\ddot{\mathbf{z}} = \mathbf{Q_u} + \mathbf{Q_c} \tag{63}$$

$$\mathbf{Q_u} = \bar{\mathbf{M}}\left[\ddot{\mathbf{z}}_{ref} + \mathbf{K}_D(\dot{\mathbf{z}}_{ref} - \dot{\mathbf{z}}) + \mathbf{K}_P(\mathbf{z}_{ref} - \mathbf{z})\right] - \mathbf{Q_c} \tag{64}$$

$$k_{Di} = 2\sqrt{k_{Pi}} \tag{65}$$

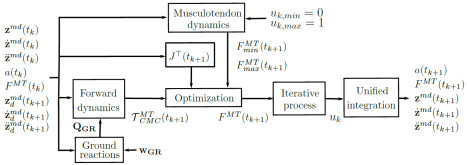

- $\mathbf{Q_u}$: the vector of the inputs provided by the controllers.
- $\mathbf{Q_c}$: vector grouping all the remaining generalized forces (centrifugal and Coriolis forces).

Multiple support

$$\mathbf{W}^* = \dot{\mathbf{z}}^{*\top}\mathbf{Q_m} \tag{66}$$

$$\mathbf{W}^* = \dot{\mathbf{y}}^{*\top}\mathbf{T} \tag{67}$$

$$\dot{\mathbf{y}} = \mathbf{B}\dot{\mathbf{z}} \tag{68}$$

$$\dot{\mathbf{z}}^{*\top}\mathbf{Q_m} = \dot{\mathbf{z}}^{*\top}\mathbf{B}^\top\mathbf{T} \tag{69}$$

$$\mathbf{B}^\top\mathbf{T} = \mathbf{Q_m} \tag{70}$$

$$\begin{pmatrix} \mathbf{W} & \mathbf{B} \\ \mathbf{B}^\top & 0 \end{pmatrix} \begin{Bmatrix} \mathbf{T} \\ \sigma \end{Bmatrix} = \begin{Bmatrix} \mathbf{W}\mathbf{T}^* \\ \mathbf{Q_m} \end{Bmatrix} \tag{71}$$

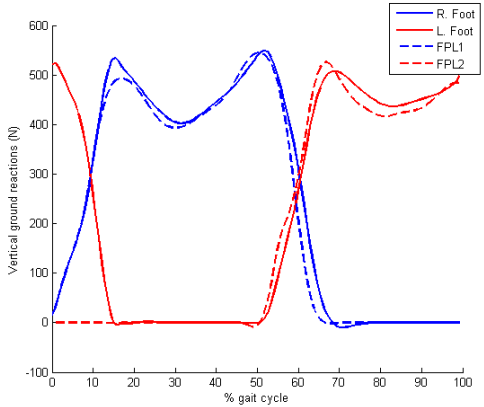

U. Lugris, J. Carlin, A. Luaces, and J. Cuadrado. Gait analysis system for spinal cord injured subjects assited by active orthoses and crutches. Journal of Multi-body Dynamics, 227, No. 4:363-374, 2013.

Splitting of the equations of motion

$$\bar{\mathbf{M}}\ddot{\mathbf{z}} = \mathbf{Q_u} + \mathbf{Q_c} \tag{72}$$

$$\begin{bmatrix} \mathbf{Q_m}^{gui} \\ \mathbf{Q_m}^{md} \end{bmatrix} = \begin{bmatrix} \bar{\mathbf{M}}_{11} & \bar{\mathbf{M}}_{12} \\ \bar{\mathbf{M}}_{21} & \bar{\mathbf{M}}_{22} \end{bmatrix} \begin{bmatrix} \ddot{\mathbf{z}}_{gui} \\ \ddot{\mathbf{z}}_{md} \end{bmatrix} - \begin{bmatrix} \mathbf{Q_c}^{gui} \\ \mathbf{Q_c}^{md} \end{bmatrix} \tag{73}$$

The equation of motion with respect to the muscle driven degrees of freedom can be obtained as follows:

$$\mathbf{Q_m}^{md} = \bar{\mathbf{M}}_{22}\ddot{\mathbf{z}}_{md} + \bar{\mathbf{M}}_{21}\ddot{\mathbf{z}}_{gui} - \mathbf{Q_c}^{md} \tag{74}$$

and simplified as:

$$\mathbf{Q_m}^{md} = \bar{\mathbf{M}}_{22}\ddot{\mathbf{z}}_{md} + H(\mathbf{z}, \dot{\mathbf{z}}, \ddot{\mathbf{z}}). \tag{75}$$

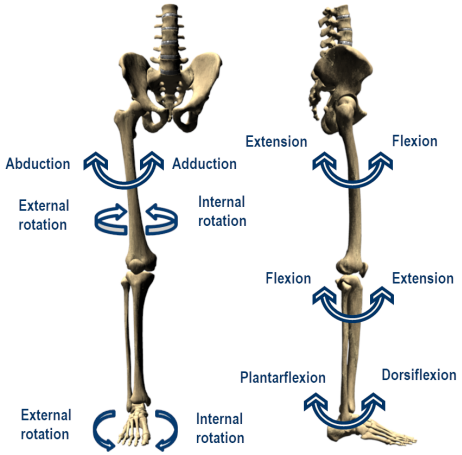

Integration using the trapezoidal rule

It's an implicit simple step integrator whose implementation results very simple. It's very appropriate for difficult problems, with rigidities high, impacts or configuration changes.

$$\mathbf{q}_{n+1} = \mathbf{q}_n + \Delta t \dot{\mathbf{q}}_n + \frac{\Delta t^2}{2} \ddot{\mathbf{q}}_n \tag{76}$$

$$\dot{\mathbf{q}}_{n+1} = \dot{\mathbf{q}}_n + \Delta t \ddot{\mathbf{q}}_n \tag{77}$$

Predictor:

$$\mathbf{q}_{n+1} = \mathbf{q}_n + \Delta t \dot{\mathbf{q}}_n + \frac{\Delta t^2}{2} \dot{\mathbf{q}}_n \tag{78}$$

$$\dot{\mathbf{q}}_{n+1} = \dot{\mathbf{q}}_n + \Delta t \ddot{\mathbf{q}}_n \tag{79}$$

Corrector:

$$\mathbf{q}_{n+1} = \mathbf{q}_n + \Delta t \dot{\mathbf{q}}_n + \frac{\Delta t^2}{4} (\ddot{\mathbf{q}}_n + \ddot{\mathbf{q}}_{pre,n+1}) \tag{80}$$

$$\dot{\mathbf{q}}_{n+1} = \dot{\mathbf{q}}_n + \frac{\Delta t}{2} t (\ddot{\mathbf{q}}_n + \ddot{\mathbf{q}}_{pre,n+1}) \tag{81}$$

Coefficient correlations R

The best pattern's correlations between muscle activation and EMG were found by cross correlation with time delay using the correlation coefficient R (Matlab's function corrcoef) and a maximum delay of 100 ms (Shourijeh et al. 2016).

Correlation coefficient R is used because there is no clear relationship between EMG amplitude and muscle force (Hof 2017).

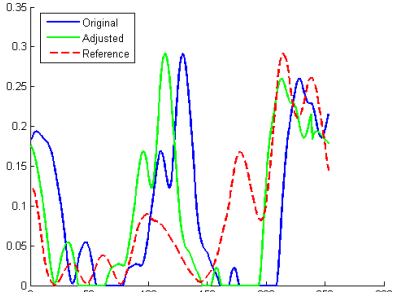

Intersegmental moments from SynO and SO-NMF

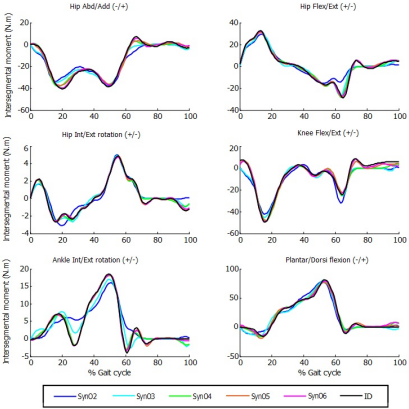

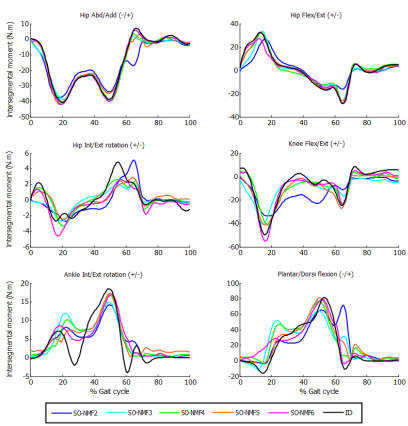

Normalized muscle activations from SynO and SO-NMF

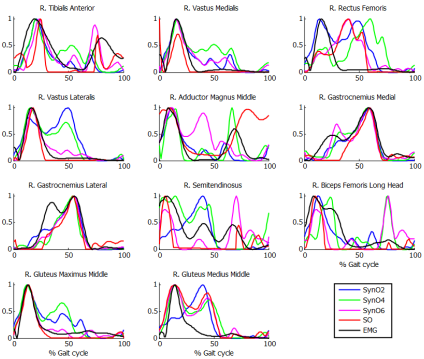

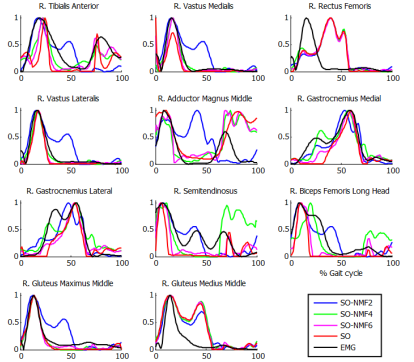

	r^2 mean values between SO and SO-NMF				
	2 Synergies	3 Synergies	4 Synergies	5 Synergies	6 Synergies
a vs. a^*	0,44	0,56	0,75	0,83	0,87